J Membrane Biol
DOI 10.1007/s00232-017-9953-2

Calcium-Induced Mitochondrial Permeability Transitions: Parameters of Ca^{2+} Ion Interactions with Mitochondria and Effects of Oxidative Agents

Nina G. Golovach[1] · Vitali T. Cheshchevik[1] · Elena A. Lapshina[1] · Tatsiana V. Ilyich[1] · Ilya B. Zavodnik[1]

Received: 29 November 2016 / Accepted: 21 February 2017

Abstract We evaluated the parameters of Ca^{2+}-induced mitochondrial permeability transition (MPT) pore formations, Ca^{2+} binding constants, stoichiometry, energy of activation, and the effect of oxidative agents, tert-butyl hydroperoxide (tBHP), and hypochlorous acid (HOCl), on Ca^{2+} -mediated process in rat liver mitochondria. From the Hill plot of the dependence of MPT rate on Ca^{2+} concentration, we determined the order of interaction of Ca^{2+} ions with the mitochondrial sites, $n = 3$, and the apparent $K_d = 60 \pm 12$ μM. We also found the apparent Michaelis–Menten constant, K_m, for Ca^{2+} interactions with mitochondria to be equal to 75 ± 20 μM, whereas that in the presence of 300 μM tBHP was 120 ± 20 μM. Using the Arrhenius plots of the temperature dependences of apparent mitochondrial swelling rate at various Ca^{2+} concentrations, we calculated the activation energy of the MPT process. ΔE_a was 130 ± 20 kJ/mol at temperatures below the break point of the Arrhenius plot (30–34 °C) and 50 ± 9 kJ/mol at higher temperatures. Ca^{2+} ions induced rapid mitochondrial NADH depletion and membrane depolarization. Prevention of the pore formation by cyclosporin A inhibited Ca^{2+}-dependent mitochondrial depolarization and Mg^{2+} ions attenuated the potential dissipation. tBHP (10–150 μM) dose-dependently enhanced the rate of MPT opening, whereas the effect of HOCl on MPT depended on the ratio of HOCl/Ca^{2+}. The apparent K_m of tBHP interaction with mitochondria in the swelling reaction was found to be $K_m = 11 \pm 3$ μM. The present study provides evidence that three calcium ions interact with mitochondrial site with high affinity during MPT. Ca^{2+}-induced MPT pore formations due to mitochondrial membrane protein denaturation resulted in membrane potential dissipation. Oxidants with different mechanisms, tBHP and HOCl, reduced mitochondrial membrane potential and oxidized mitochondrial NADH in EDTA-free medium and had an effect on Ca^{2+}-induced MPT onset.

Keywords Liver mitochondria · Calcium · Mitochondrial permeability transition · Tert-butyl hydroperoxide · Hypochlorous acid

Abbreviations

MPT	Mitochondrial permeability transition
CypD	Cyclophilin D
CsA	Cyclosporin A
ANT	Adenine nucleotide (ADP/ATP) transporter
VDAC	Voltage-dependent anion channel
ROS	Reactive oxygen species
tBHP	Tert-butyl hydroperoxide
HOCl	Hypochlorous acid
FCCP	Carbonyl cyanide p-trifluoro-methoxyphenyl hydrazone
MCU	Mitochondrial Ca^{2+} uniporter

Introduction

Mitochondria are dynamic and plastic organelles involved in a number of crucial metabolic processes, such as energy metabolism, ATP synthesis, the tricarboxylic acid cycle, and β-oxidation of fatty acids (Duchen 2004; Patergnani et al. 2011; Jonas 2015). Mitochondria are also one of the major components of calcium signaling, capable of modulating both the amplitude and the spatio-temporal patterns

✉ Ilya B. Zavodnik
zavodnik_il@mail.ru

[1] Department of Biochemistry, Yanka Kupala State University of Grodno, Blvd. Len. Kom. - 50, 230030 Grodno, Belarus

Published online: 01 March 2017

of Ca^{2+}-signals, and the major site for Ca^{2+} sequestration (Patergnani et al. 2011). Cellular and mitochondrial Ca^{2+}-ion homeostasis is fundamental for cell metabolism¸ proliferation, differentiation, gene activation, as well as cell survival and death (Patergnani et al. 2011; Rizzuto et al. 2012). The main role of mitochondrial Ca^{2+} is stimulation of Ox-Phos enzymes and matrix dehydrogenases (Rizzuto et al. 2012). Furthermore, Ca^{2+} ions can be determinants for the rates of mitochondrial reactive oxygen species (ROS) release (Armstrong et al. 2004).

Mitochondria are major cellular targets of oxidative stress. It is widely known that oxidative stress and disturbance in Ca^{2+}-homeostasis can cause bioenergetic failure by activation of the mitochondrial inner membrane permeability transition (MPT) (Orrenius et al. 2003). The MPT pore is a non-selective calcium-sensitive channel that allows non-selective diffusion of solutes (<1500 Da) across the membrane and plays a crucial role in cell death (Armstrong et al. 2004; Orrenius et al. 2003; Kowaltowski et al. 2001). Opening of this high conductance cyclosporine A (CsA)-sensitive, Ca^{2+}- mediated pore causes both collapse of the membrane potential, large amplitude of mitochondrial swelling, membrane rupture, and release of sequestered Ca^{2+}, small metabolites, and apoptogenic signal molecules (Orrenius et al. 2003). MPT opening also leads to mitochondrial uncoupling, pyridine nucleotide, and ATP depletion, disruption of ionic homeostasis, and induces ROS productions at the level of Complex I (Batandier et al. 2004, Alaviana et al. 2014; Halestrap et al. 1997). Petrosillo et al. (2004) found that Ca^{2+}-induced ROS production and cardiolipin peroxidation promote cytochrome *c* release from rat liver mitochondria via MPT-independent (at low extramitochondrial Ca^{2+} level—2 μM) and MPT-dependent mechanisms (at high extramitochondrial Ca^{2+} level—20 μM). Ca^{2+}-induced MPT pore formations participate in the pathophysiology of many diseases (Halestrap et al. 1997). Inhibitors of MPT might have a therapeutic potential and should be useful in prevention of mitochondria-associated cytotoxic events, such as cardiac ischemia–reperfusion injury, stroke, and excitotoxicity (Baranov et al. 2008).

The crosstalk between Ca^{2+} and ROS signaling pathways within mitochondria is the topic of great interest (Feissner et al. 2009). tert-Butyl hydroperoxide (tBHP), an analogue of organic lipid hydroperoxides, is widely used as an oxidative agent in studies evaluating the sensitivity of cells and cellular organelles to oxidative damage (Bellomo et al. 1982; Kennedy et al. 1992; Drahota et al. 2005). The earlier work of Lapidus and Sokolove (1994) showed that MPT of isolated rat liver mitochondria was triggered using Ca^{2+}, tBHP and Pi, agents acting via different mechanisms. Numerous works (Byrne et al. 1999; Drahota et al. 2005; Kriváková et al. 2007; Zavodnik et al. 2013) have shown that peroxidative damage by tBHP results in inhibition of oxidative phosphorylation of both isolated mitochondria and permeabilized cells due to uncoupling of respiration and damage of the electron transport chain complexes, as well causes an early increase of mitochondrial matrix free Ca^{2+}, enhanced mitochondrial ROS generation and NAD(P)H oxidation, followed by onset of MPT. It was shown that Complex I containing sulfur–iron clusters is more sensitive to peroxidative damage in comparison with flavoprotein-containing Complex II (Drahota et al. 2005).

It was shown that another oxidant, HOCl, a highly toxic agent, produced in the sites of inflammation, induced MPT, rapid mitochondrial swelling, and collapse of the membrane potential of isolated mitochondria or mitochondria in whole cells (Whiteman et al. 2005; Yang et al. 2012). HOCl at concentrations of 50–200 μM caused rapid necrotic cell death in human monocyte-derived macrophages without caspase-3 activation via triggering an increase in cytosolic Ca^{2+} (calcium entered cytoplasm from both extracellular and intracellular sites), whereas elevated calcium triggered calpain-dependent MPT pore formation, leading to membrane potential and cellular ATP loss (Yang et al. 2012). Similarly, in HEPG2 and human fetal liver cells, HOCl (15–125 μM) caused MPT pore formation, triggering caspase-3 activation through cytochrome *c* release. HOCl –induced MPT formation leads to apoptosis or necrosis and explains the mechanism of cell death at sites of inflammation (Whiteman et al. 2005). These effects of HOCl are induced at physiological concentrations of this effector generated by activated neutrophils (20–200 μM) (Davies et al. 1993; Favero et al. 1998; King and Jefferson 1997).

Despite numerous investigations, the nature and molecular composition of MPT pores as well as the mechanism of formation remain controversial (Patergnani et al. 2011; Rizzutto et al. 2012; Richardson and Halestrap 2016; Santo-Domingo and Demaurex 2010). The aim of the present work was further elucidation of the parameters of Ca^{2+}-induced MPT, the steps of the Ca^{2+}-mediated process, Ca^{2+} binding constants, stoichiometry, energy of activation, and the interrelationships of calcium ions and oxidants, tBHP, and HOCl, at the onset of mitochondrial permeability transition.

Materials and Methods

Chemicals

tBHP, HOCl, calcium chloride dehydrate, succinic acid disodium salt hexahydrate, L-glutamic acid sodium salt, L-malic acid sodium salt, safranin O, carbonyl cyanide p-trifluoro-methoxyphenyl hydrazone (FCCP), ADP, and cyclosporine A (CsA) were purchased from Sigma-Aldrich Chemie GmbH (Steinheim, Germany). All other

reagents were purchased from POCh (Gliwice, Poland) and Reakhim (Moscow, Russia) and were of analytical grade. All solutions were made with water purified in the Milli-Q system.

Isolation of Rat Liver Mitochondria

Mitochondria were isolated by the standard procedure of differential centrifugation from the rat liver by the method of Johnson and Lardy (1967). The mitochondrial pellet was resuspended in the buffer to an approximate protein concentration of 35–40 mg/ml. The protein concentration was determined by the method of Lowry et al. (1951). The isolation medium contained 0.125 M KCl, 0.05 M sucrose, 0.01 M Tris-HCl, 0.0025 M KH_2PO_4, 0.005 M $MgSO_4$ (or without Mg^{2+}) with 0.0005 M EDTA (EDTA-containing) or without EDTA (EDTA-free medium), pH 7.4.

Mitochondrial Swelling

Ca^{2+}-induced swelling of respiring mitochondria was analyzed as changes of mitochondrial suspension light scattering determined from the absorbance changes of the suspension at 520 nm (Petronilli et al. 1993a) at 25°C using a buffer containing 0.25 M sucrose, 0.02 M Tris-HCl, and 0.001 M KH_2PO_4, pH 7.4. Isolated mitochondria (0.5 mg of protein/ml) were added to the media, containing respiratory substrate (5 mM succinate). After 5 min, Ca^{2+} ions were added and the rate (ΔD^{520}/min) of the termination phase of the swelling was measured. The rate of the decrease in light scattering was used to determine the extent of mitochondrial pore opening. At the end of the measurements, uncoupler FCCP (0.5 µM) was added to mitochondria to control the finishing of the MPT process. The representative curves of mitochondrial swelling (Fig. 1a) corresponded to the curves of other authors (Baranov et al. 2008; Whiteman et al. 2005). In the case of evaluation of the effect of CsA on mitochondrial swelling and potential changes,

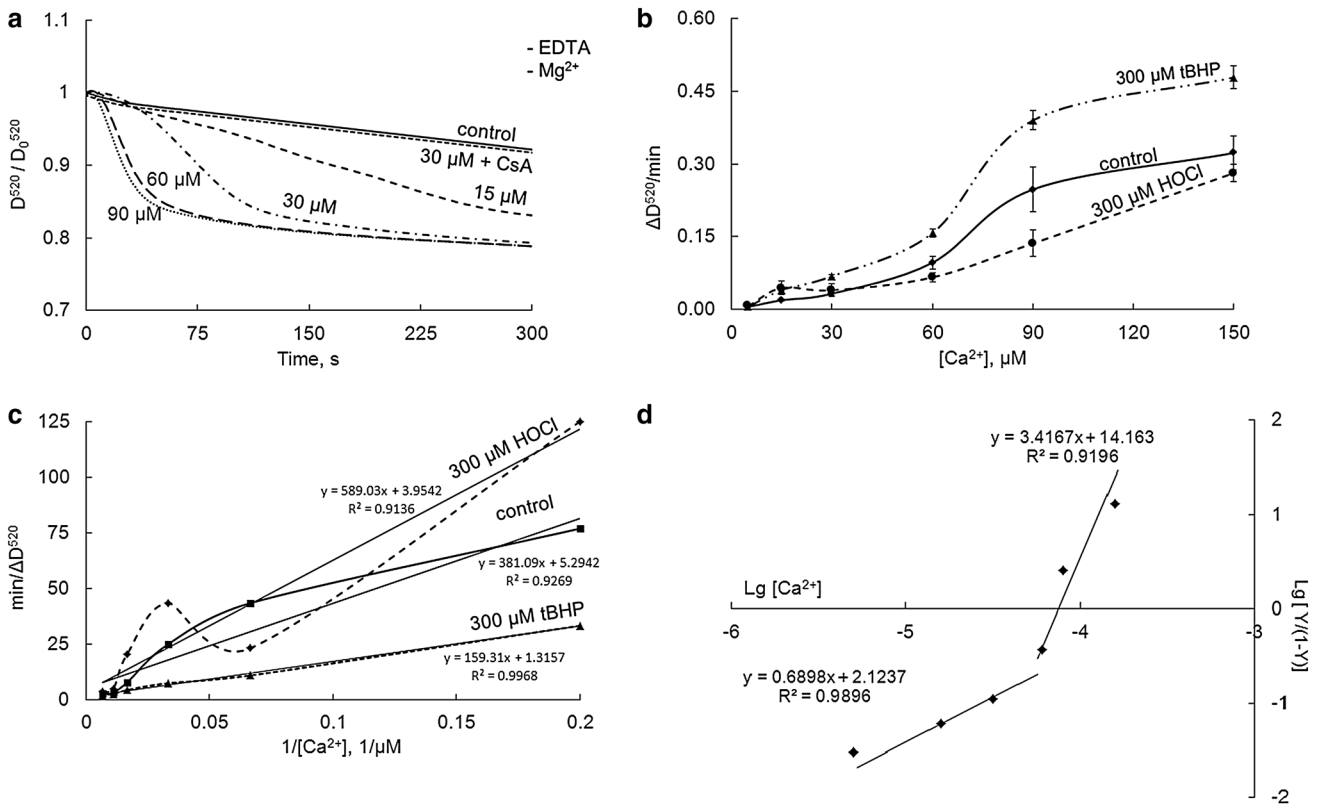

Fig. 1 Dependence of the rate of Ca^{2+} -induced MPT on Ca^{2+} ion concentration: effects of CsA and oxidative agents (300 µM), tBHP and hypochlorous acid. **a** Representative curves of rat liver mitochondria swelling at different concentrations of exogenous Ca^{2+} (15 µM, 30 µM, 30 µM + CsA, 60 µM, 90 µM) in EDTA-free medium registered as changes of mitochondria (0.5 mg/ml) suspension absorption at 520 nm; **b** dependences of mitochondrial swelling rate v (ΔD^{520}/min) on Ca^{2+} concentration in the absence and in the presence of tBHP (300 µM) or HOCl (300 µM); **c** the same dependences represented as the Lineweaver–Burk plots (or double reciprocal plots); **d** the Hill plot of the dependence of mitochondrial swelling rate on Ca^{2+} concentration

mitochondria were preincubated in the presence of 2 μM CsA at 25°C for 30 min.

Mitochondria NAD(P)H Measurements

Mitochondrial NAD(P)H oxidation was measured by a kinetic method using an excitation/emission pair of 340/465 nm and a Perkin-Elmer LS55 spectrofluorimeter (Great Britain) according to the established method (Bartolomé and Abramov 2015). Measurement of NAD(P)H level was performed at 25°C during 20 min using 5 mM L-glutamate and 2 mM L-malate as substrates. Isolated mitochondria were added to the EDTA-free media (0.05 M sucrose, 0.01 M Tris-HCl, 0.125 M KCl, 2.5 mM KH_2PO_4, 5 mM $MgSO_4$, pH 7.4) at a concentration of 0.3 mg of protein/ml and after 5 min effectors (Ca^{2+}, tBHP, or HOCl) were introduced. At the end of the measurements the uncoupler FCCP (0.5 μM) was added to mitochondria.

Mitochondrial Membrane Potential Measurements

Mitochondrial membrane potential was detected with a Perkin-Elmer LS55 spectrofluorimeter (Great Britain), using the fluorescent dye safranin O (8 μM) at λex/λem 495/586 nm (Akerman and Wikström 1976; Moore and Bonner 1982) and the buffer containing 0.05 M sucrose, 0.01 M Tris-HCl, 0.125 M KCl, 2.5 mM KH_2PO_4, 5 mM $MgSO_4$ (or without Mg^{2+}), and 0.5 mM EDTA or without EDTA (EDTA-free medium), pH 7.4. Measurement of potential was performed at 25°C using 5 mM succinate as substrate. Isolated mitochondria were added to the media at a concentration of 0.3 mg of protein/ml and after 5 min effectors (Ca^{2+}, tBHP, or HOCl) were added. The positively charged dye accumulated in mitochondria depending on their potential, with the intramitochondrial dye accumulation resulting in fluorescence quenching. The mitochondrial membrane potential values (mV) were determined using a calibration plot which represented the dependence of safranine O fluorescence intensity on the mitochondrial membrane potential value, calculated according to the Nernst equation:

$$\Delta\Psi = 60\log\left[K^+\right]_{out}/\left[K^+\right]_{in} \quad (\text{mV}),$$

where the $[K^+]_{in}$ is the intramitochondrial potassium concentration (120 mM) and the $[K^+]_{out}$ is the extramitochondrial potassium concentration in the medium that varies from 0 to 20 mM (Akerman and Wikstrom 1976 ; Moore and Bonner 1982). For calibration, the membrane potential values were changed by the varying extramitochondrial potassium concentration in the medium in the presence of ionophore valinomycin (0.28 μM). Complete depolarization of mitochondria to calibrate the dye fluorescence was achieved by addition of FCCP (0.5 μM). To express the dependence of mitochondrial potential on calcium concentration, we used the value of potential change per min (mV/min).

Statistical Analysis

The results were expressed as the means of four to five replicates ± SD and the statistical analysis was conducted using the analysis of variance (ANOVA). We used the standard Student's *t* test for the comparison of the raw and transformed data showing no departures from normality (according to Shapiro–Wilk's test).

Results

Parameters of Ca^{2+} Ion-Induced MPT

In isolated rat liver mitochondria, exogenous Ca^{2+}-ions dose-dependently induced MPT onset which was registered by mitochondria swelling (Fig. 1a shows the representative swelling curves). CsA (2 μM) completely prevented absorbance changes (Fig. 1a). The swelling rate ($v = \Delta D^{520}$/min) depended on the added Ca^{2+} concentration, temperature, and the presence of the oxidants (Figs. 1, 2). Using the Lineweaver–Burk plot of the dependence of the reciprocal apparent swelling rate (min/ΔD^{520}) on the reciprocal Ca^{2+} concentration (1/[Ca^{2+}]), we calculated the apparent Michaelis–Menten constant, K_m, of Ca^{2+} ions interaction with rat liver mitochondria sites (or Ca^{2+} concentration corresponding to half the maximal swelling rate) (Fig. 1c). The apparent K_m was calculated to be 75 ± 20 μM. Figure 1d shows the dependence of the swelling rate on Ca^{2+} concentration using the Hill equation:

$$\lg\left[Y/(1-Y)\right] = n\lg\left[Ca^{2+}\right] - n\lg K_d,$$

where Y is the fraction of the ligand-binding sites in mitochondria that were occupied by the ligand (Ca^{2+}) at the corresponding Ca^{2+} concentration (determined as $Y = v_{[Ca2+]}/v_{max}$, the ratio of the swelling rate $v_{[Ca2+]}$ at the appropriate calcium concentration [Ca^{2+}] to the maximal swelling rate v_{max}), n is the Hill coefficient which characterizes the degree of binding cooperativity, and K_d is the dissociation constant of ligand binding to mitochondria sites. If the cooperativity is full, the Hill coefficient equals the number of ligand-binding sites. The Hill plot intersects the abscissa axis at half-saturation concentration of the ligand (or K_d point), which reflects the affinity of the mitochondria for the ligand. In the range of 30–150 μM Ca^{2+} ions, the apparent K_d = 60 ± 12 μM (this value is close to the K_m value, determined from the Lineweaver–Burk plot) and the Hill

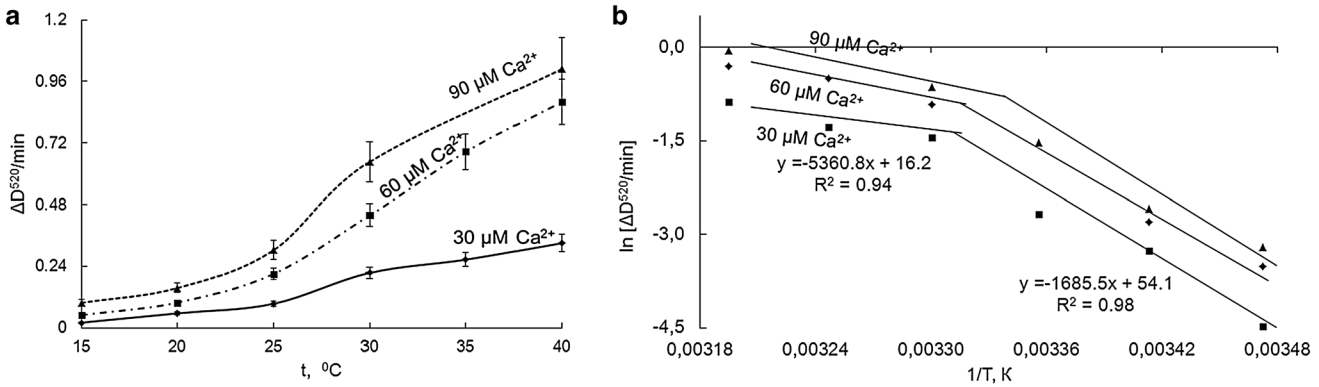

Fig. 2 Temperature dependences of MPT process. Temperature dependences of the MPT onset at different Ca^{2+} concentrations (**a**); the same dependences represented as Arrhenius plots (**b**)

coefficient is equal to $n = 3$, and $n = 1$ at lower Ca^{2+} concentrations, in accordance with the theory of the Hill equation.

Figure 2 represents the temperature dependence of the apparent mitochondria swelling rate at various Ca^{2+} concentrations. Using these dependences and the Arrhenius equation, we determined the activation energy of the MPT process:

$$v = A\, e^{-\Delta Ea/RT},$$

where v is the swelling rate at the temperature T (K), A is the pre-exponential factor, R is the Gas constant, and ΔEa is the activation energy of Ca^{2+}-induced swelling. The Arrhenius plots at different Ca^{2+} concentrations showed a break at 30–34 °C (Fig. 2b). The activation energies of the MPT onset were found to be $\Delta Ea = 130 \pm 20$ kJ/mol at lower temperatures and $\Delta Ea = 50 \pm 9$ kJ/mol at the temperatures above the inflection point.

The exposure of isolated mitochondria to exogenous Ca^{2+} resulted in rapid mitochondrial membrane depolarization in EDTA-free medium, as was measured using the potential-sensitive dye safranin O (Fig. 3a, b), and in fast depletion of mitochondrial NAD(P)H, as was analyzed by the method of NAD(P)H autofluorescence (Fig. 3c). Under these conditions, CsA pretreatment markedly prevented membrane potential loss (Fig. 3a). In accordance with the previous observations, Mg^{2+} -ions inhibited Ca^{2+}-induced membrane depolarization (Fig. 3b). As Fig. 4 shows, Ca^{2+}-induced membrane potential dissipation and NADH oxidation are parallel processes.

Effect of tBHP and HOCl on Ca^{2+}-Induced MPT

The preliminary exposure of isolated mitochondria to tBHP dose-dependently increased the rate of Ca^{2+} -induced mitochondria swelling (Fig. 1b). Using the Lineweaver–Burk plot of dependence of swelling rate on Ca^{2+} concentration in the presence of 300 μM tBHP, we showed that the oxidant increased the apparent K_m and the v_{max} for Ca^{2+} -induced mitochondrial swelling (Fig. 1c). The apparent K_m for Ca^{2+} interactions with mitochondria in the presence of 300 μM tBHP was calculated to be equal to 120 ± 20 μM. One can suggest that the mitochondria exposure to the oxidant elevated the number of Ca^{2+} binding sites. Figure 5a represents the dependence of Ca^{2+} -induced mitochondrial swelling rate (ΔD^{520}/min) on tBHP concentration in EDTA-free medium in the presence of 30 μM of Ca^{2+}. From the Lineweaver–Burk plot of this dependence, we calculated the apparent Michaelis–Menten constant, K_m, of the oxidant interaction with mitochondria in the swelling reaction, and the K_m was found to be 11 ± 3 μM (Fig. 5b). In the absence of exogenous calcium in EDTA-free medium, tBHP-induced slow mitochondrial membrane depolarization (Fig. 6a), as was measured using a potential-sensitive probe, and NAD(P)H depletion (Fig. 6c) evaluated by a decrease of NAD(P)H fluorescence. In the presence of 0.5 mM EDTA, tBHP did not induce any changes in the membrane potential (Fig. 6b). Thus, the mitochondrial effect of tBHP depended on the presence of endogenous Ca^{2+} ions in the media. Interestingly, at low oxidant concentrations (0.02 mM), the NADH level in mitochondria partially reversed (Fig. 6c).

The second oxidant, HOCl, exerted a considerable effect on Ca^{2+} -induced MPT (Fig. 1b, c). The effect of HOCl depended on the ratio of HOCl/Ca^{2+}. HOCl (at a constant concentration of 300 μM HOCl) increased the rate of Ca^{2+}–induced mitochondria swelling at low concentrations of Ca^{2+} ions (15 μM) and decreased this parameter at higher Ca^{2+} concentrations (60–150 μM) (Fig. 1b) in comparison with the control experiments. In EDTA-free medium, HOCl induced slow time-dependent mitochondrial membrane depolarization (Figs. 7a, 8) and NADH depletion (Figs. 7c, 8), which were parallel processes. EDTA (0.5 mM) significantly prevented HOCl-mediated decrease of mitochondrial membrane potential (Fig. 7b).

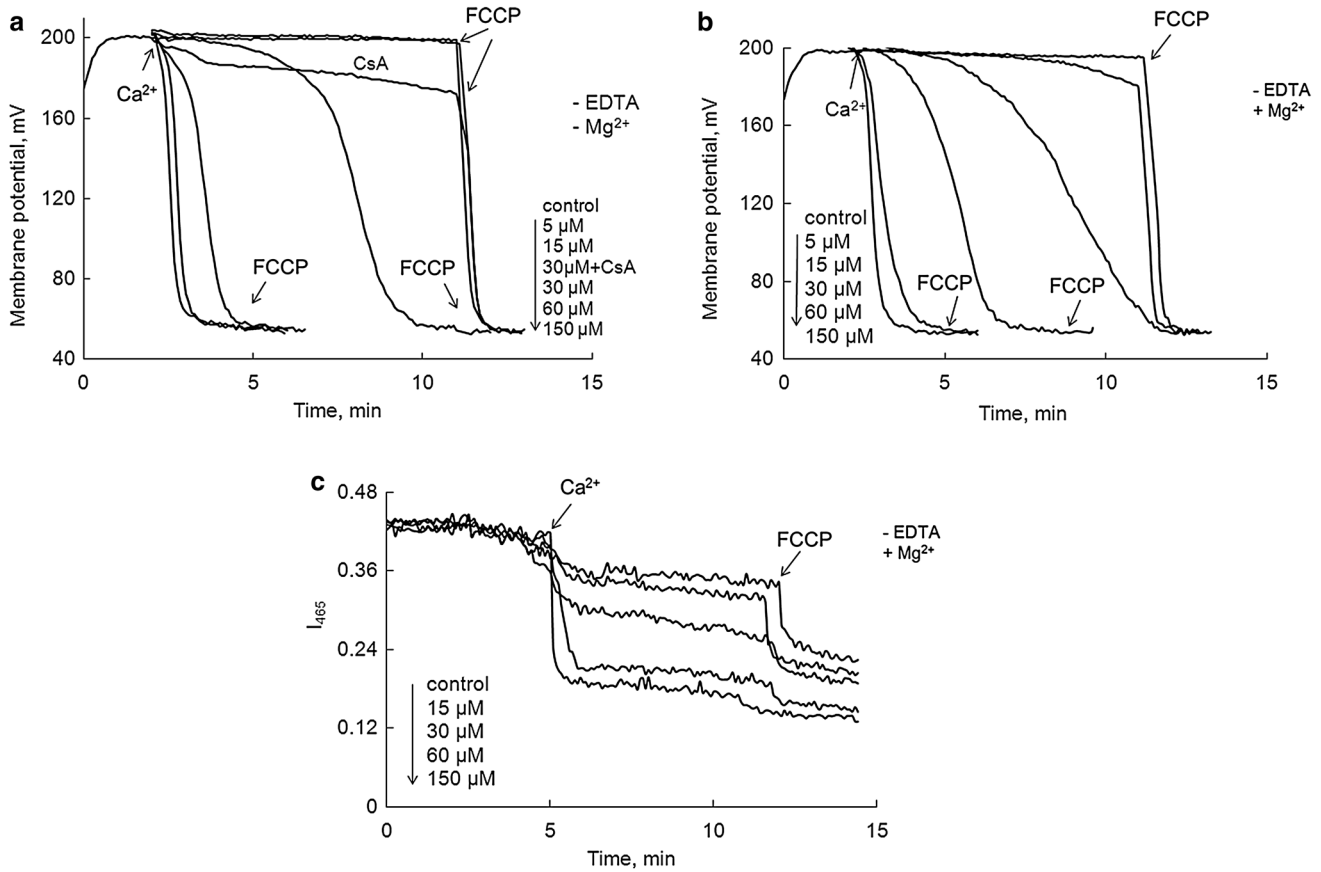

Fig. 3 Representative curves of Ca^{2+} -induced mitochondrial potential dissipation and NADH depletion. Ca^{2+} ions dissipate the membrane potential (**a, b**) and deplete NADH (**c**) of rat liver mitochondria (0.3 mg/ml) in EDTA-free media in the absence (**a**) and in the presence of 0.5 mM Mg^{2+} (**b, c**). The *arrows* indicate the additions of Ca^{2+} and FCCP (0.5 μM). The mitochondrial membrane potential was detected using the fluorescent dye safranin O (8 μM) at λex/λem 495/586 nm at 25°C and 5 mM succinate as substrate. Mitochondrial NADH oxidation was measured using an excitation/emission pair of 340/465 nm and 5 mM L-glutamate and 2 mM L-malate as substrates at 25°C

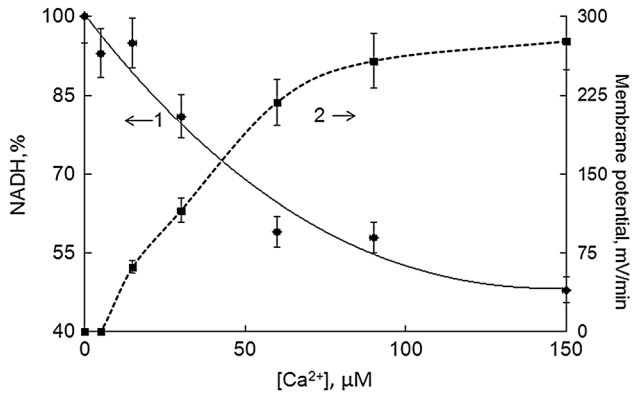

Fig. 4 Effect of Ca^{2+} on the rate of NADH oxidation and membrane potential dissipation. Dependences of the rates of rat liver mitochondrial NADH oxidation (1) and membrane potential dissipation (2) on Ca^{2+} concentrations in EDTA-free media, pH 7.4, 25 °C (for details see the legend to Fig. 3). NADH level was measured after 5 min following Ca^{2+} addition

Discussion

Possible mechanisms of Ca^{2+} overload-induced mitochondria dysfunction include Ca^{2+}-stimulated increase in mitochondrial metabolic rate, nitric oxide production, cardiolipin peroxidation, MPT pore opening, and Ca^{2+}-calmodulin-dependent protein kinases activation (Peng and Jou 2010; Battaglia et al. 2010; Petrosillo et al. 2004).

A mitochondrial Ca^{2+} channel, known as mitochondrial Ca^{2+} uniporter (MCU), drives the rapid and massive input of Ca^{2+} ions into mitochondria. The uniporter operates at high, micromolar cytosolic Ca^{2+} concentrations (Pandya et al. 2013). Mitochondria can also take up Ca^{2+} at low, nanomolar cytosolic concentrations by electrogenic 1:1 mitochondrial Ca^{2+}/H^{+} antiporter (Letm1) that is bidirectional and can extrude Ca^{2+} from the matrix (Patergnani et al. 2011; Rizzuto et al. 2012; Santo-Domingo and Demaurex 2010).

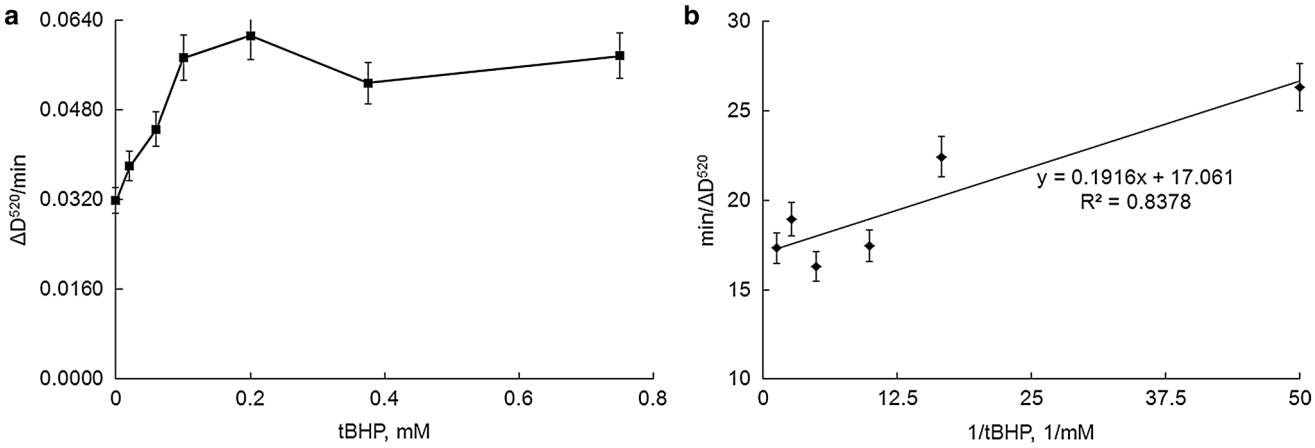

Fig. 5 Effect of tBHP on mitochondria swelling Dependence of the rate of Ca^{2+}-induced rat liver mitochondria swelling on tBHP concentration in EDTA-free medium, 30 μM Ca^{2+}, 25 °C (**a**) (for details see the legend to Fig. 1); the same dependence represented as the Lineweaver–Burk plot (**b**)

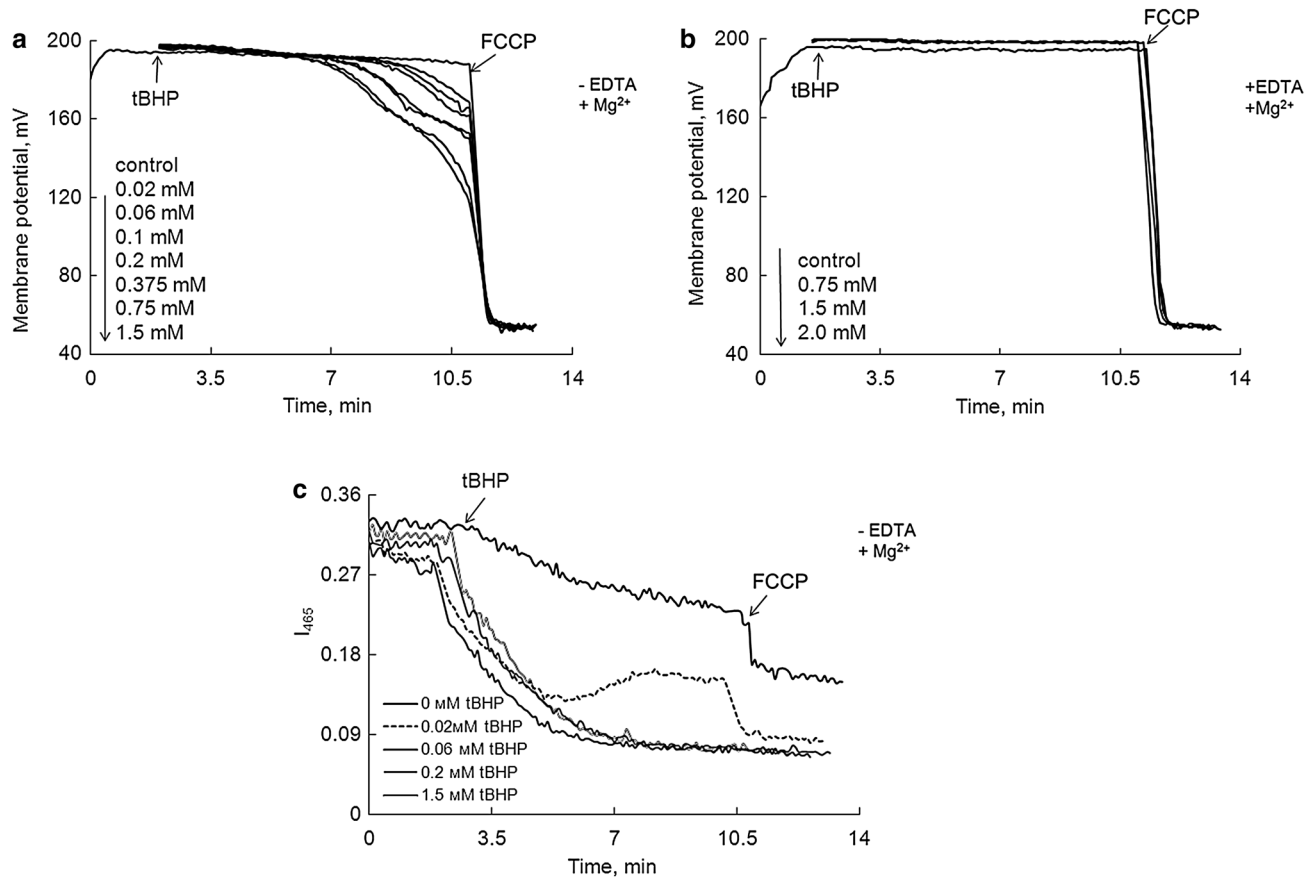

Fig. 6 Representative curves of tBHP-induced mitochondrial membrane potential dissipation and NADH oxidation. Time-dependences of tBHP-induced dissipation of mitochondrial membrane potential (**a, b**) and NADH oxidation (**c**) in EDTA-free (**a, c**) and EDTA-containing (**b**) media in the absence of Ca^{2+} addition. The *arrows* indicate tBHP and FCCP additions (for details see the legend to Fig. 3)

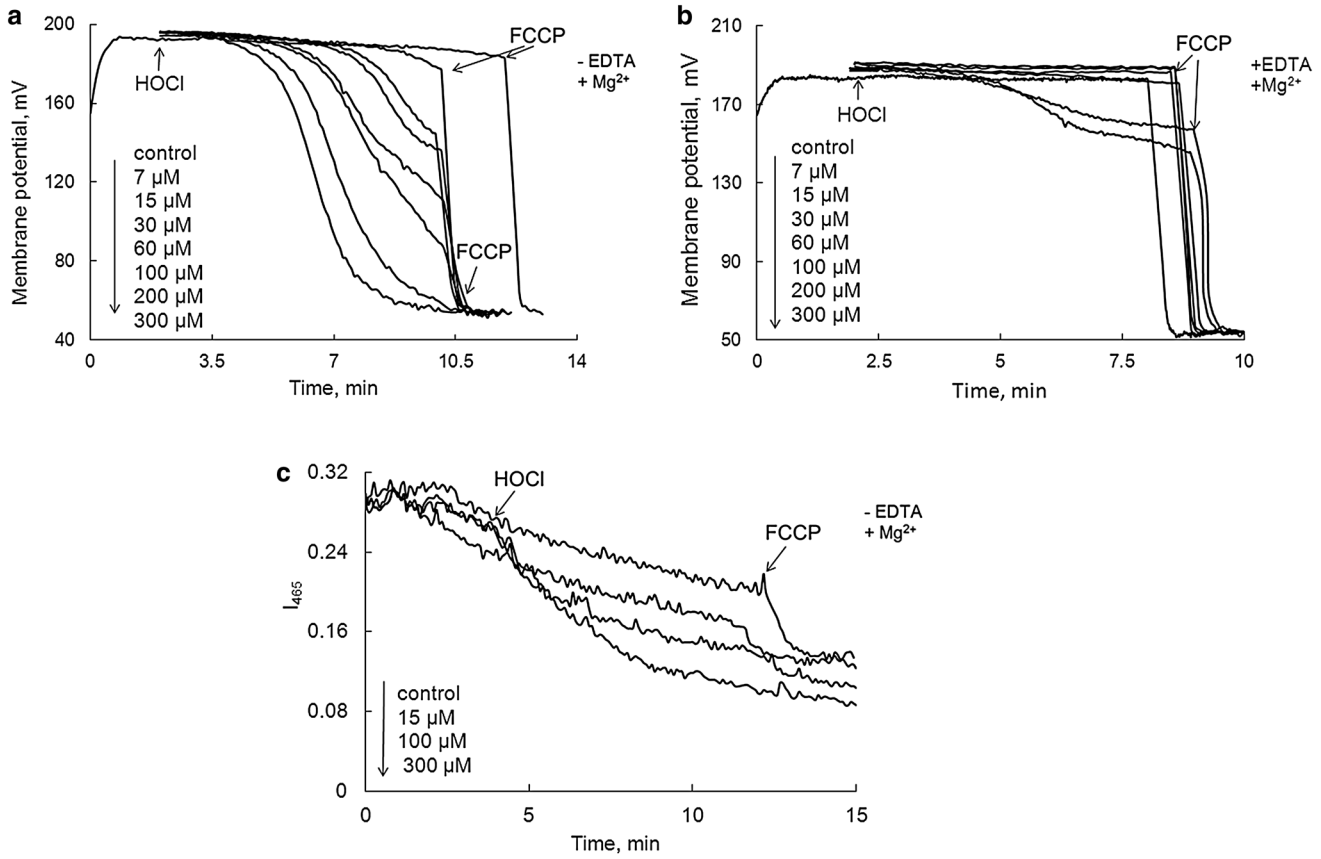

Fig. 7 HOCl-induced mitochondrial membrane potential dissipation and NADH oxidation. In the absence of Ca^{2+} addition, hypochlorous acid dissipates mitochondrial membrane potential (**a, b**) and oxidizes mitochondrial NADH (**c**) in EDTA-free (**a, c**) and EDTA-containing (**b**) media (for details see the legend to Fig. 3)

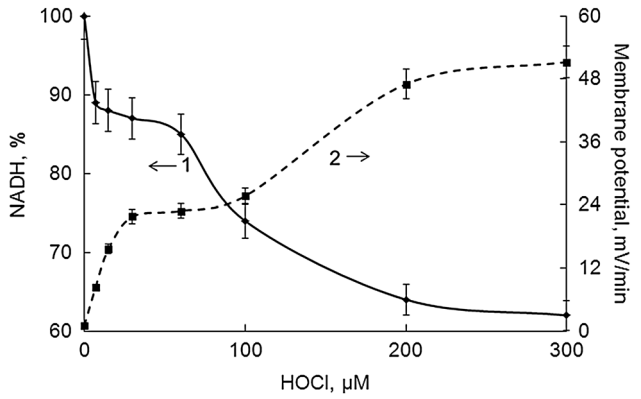

Fig. 8 Effect of HOCl on mitochondrial NADH depletion and membrane depolarization. Dependences of the rates of mitochondrial NADH depletion (1) and membrane depolarization (2) on HOCl concentration in EDTA-free medium, pH 7.4, 25 °C in the absence of Ca^{2+} addition (for details see the legend to Fig. 3). NADH level was measured after 5 min following HOCl addition

Many earlier studies have considered the MPT to be due to the formation of a preformed pore complex between the mitochondrial inner and outer membranes (McStay et al. 2002), an alternative view has been that the MPT is not a result of opening of a preformed pore, but is due to increased membrane permeability caused by oxidative damage to membrane proteins including the adenine nucleotide translocase (ANT) (Kowaltowski et al. 2001). According to the earlier models, MPT pore would be a multiprotein complex spanning both (outer and inner) mitochondrial membranes and comprising ANT, VDAC, and peripheral benzodiazepine receptor, an OMM protein nowadays called TSPO, matrix protein cyclophilin D (CypD) as well as hexokinase and Bcl-2 proteins (Zamzami and Kroemer 2001). Cyps are highly conserved ubiquitous proteins which possess peptidyl-prolyl-*cis-trans* isomerase activity. Matrix CypD acts as key regulator of MPT, enhancing its sensitivity to Ca^{2+}, and as the site of the action of inhibitor of MPT pore opening, CsA (Richardson and Halestrap 2016). The important feature of the mammalian PTP is its modulation by redox effectors, while a more oxidized state favors PTP opening. Recently, the Bernardi P. group

suggested that under conditions of oxidative stress, dimers of the F_0F_1-ATP synthases of mammalian mitochondria, yeast, and Drosophila can be turned into Ca^{2+}-dependent channels whose electrophysiological properties match those of the corresponding MPT pores (Bernardi et al. 2015; Bernardi and Di Lisa 2015). Thus, MPT transforms F_0F_1-ATP synthases from an energy-conserving into an energy-dissipating device and plays an important role in cellular pathophysiology (Giorgio et al. 2013). Membrane potential and matrix pH are the key modulators of MPT pores and are also the key regulators of ATP synthase. The pores play a potential role as Ca^2 release channels. Channel openings are favored by thiol oxidation and inhibited by adenine nucleotides and Mg^{2+} (Bernardi 2013).

On the other hand, Halestrap and coworkers suggested that the MPT pore might be formed at an interface between ANT (in "c" conformation) and the phosphate carrier (P_iC) and both of which can bind CypD (Richardson and Halestrap 2016; Halestrap 2014). It was suggested that the ANT usually plays a regulatory role in MPT onset rather than provides the transmembrane pore component and that a calcium-triggered conformational change of the mitochondrial P_iC, facilitated by CypD, induces pore opening (Leung and Halestrap 2008). Ca^{2+} may act through binding to annular cardiolipin. Jonas et al. (2015) suggested that the c-subunit of F_1F_0 ATP synthase is the main molecular component of the MPT pore. It was shown that the purified reconstituted c-subunit ring of the membrane portion F_O of F_1F_O ATP synthase forms a voltage-sensitive channel whose persistent opening leads to rapid and uncontrolled depolarization of the inner mitochondrial membrane (Alaviana et al. 2014). It seemed possible that Bcl-2 family proteins could form part of a large protein complex that regulates MPT and cell death.

From a kinetic point of view, at least three distinct phases must be resolved during the MPT in` isolated rat liver mitochondria: (1) initial intake of Ca^{2+}; (2) a „lag" phase during which Ca^{2+}-induces a series of processes (pre-swelling MPT induction); (3) a positive feedback autocatalytic propagation or „termination" phase during which pore opening, mitochondria swelling, and sequestered Ca^{2+} release take place (Baranov et al. 2008).

In the current study, we have estimated the parameters (stoichiometry, affinity, activation energy) characterizing calcium interactions with mitochondria during MPT and have demonstrated the effects of oxidants on this process. The apparent K_m for Ca^{2+} interactions with mitochondrial sites (75 ± 20 μM, as was calculated from the Michaelis–Menten plot of the dependence of MPT rate on Ca^{2+} concentration), and the apparent K_d (60 ± 12 μM, as was calculated from the Hill plot) were higher than those for the mitochondrial uniporter (MCU), while experiments on permeabilized cells reported the K_d of 10 μM Ca^{2+} for the uniporter (Patergnani et al. 2011). The order of the reaction of Ca^{2+} ions with the mitochondrial membrane was calculated to be equal to $n = 3$ (the Hill coefficient). It means that three Ca^{2+} ions cooperatively participate in the pore formation. The activation energy of Ca^{2+} -induced MPT at temperatures below the break point of the Arrhenius plot ($E_a = 130 \pm 20$ kJ/mol) corresponds to the activation energy of the protein denaturation process. One can suggest that mitochondrial pore formation is driven by denaturation transition of one of the mitochondrial membrane proteins. The break of the Arrhenius plot at 30–34 °C may reflect mitochondrial membrane transformations due to phase transition of membrane lipids. The activation energy of the MPT process at higher temperatures ($E_a = 50 \pm 9$ kJ/mol) is in line with the value of enthalpy of lipid bilayer phase transition (20–50 kJ/mol) (Marsh 1992). As we showed, the activation energy of the MPT did not depend on Ca^{2+} concentration. The elevation of Ca^{2+} concentration increased the rate of the MPT but it did not change the energy threshold of this process. Ca^{2+}-induced dissipation of the mitochondrial membrane potential and NADH oxidation were related to the MPT onset. It was shown that the decrease in the transmembrane mitochondrial potential stimulated MPT and increased transmembrane potential prevented MPT (Kowaltowski et al. 2001).

In our experiments, prevention of the pore formation by CsA (Fig. 1a) considerably inhibited Ca^{2+}-induced membrane depolarization (Fig. 3a). Similarly, Hawkins et al. (2010) showed earlier that CsA (5 μM) pretreatment of permeabilized rat pulmonary microvascular endothelial cells significantly blunted Ca^{2+}-dependent mitochondrial depolarization that occurred via the MPT pore opening. Yang et al. showed for human monocyte-derived macrophages that blocking HOCl-induced MPT pore formation with CsA prevented the loss of mitochondrial membrane potential and cell death (Yang et al. 2012). We suggested that mitochondrial depolarization occurred via Ca^{2+}-stimulated mitochondrial membrane permeabilization. However, in their earlier works, Petronilli et al. (1993a, b) emphasized that MTP opening is the consequence rather than the cause of membrane depolarization. The membrane depolarization is both necessary and sufficient to trigger pore opening. Similarly, it was shown earlier that the oxidant tBHP caused a collapse of the mitochondrial membrane potential, which preceded the onset of mitochondrial swelling. CsA dramatically slowed swelling induced by tBHP without altering prooxidant-induced depolarization (Kushnareva and Sokolova 2000).

The other cause of membrane potential loss in the presence of exogenous Ca^{2+} is the Ca^{2+}-dependent direct inhibition of the mitochondrial respiration (Pandya et al. 2013). Similarly, the movement of Ca^{2+} into energized mitochondria should directly decrease membrane potential.

Mg^{2+} partially inhibited the dissipative effect of Ca^{2+} (in EDTA-free medium). It is well-known that Mg^{2+} inhibits Ca^{2+}-induced MPT, probably because of the competition for binding at the Ca^{2+} transport site of the uniporter (Baranov et al. 2008). Mg^{2+} interferes with Ca^{2+} in the reaction of Ca^{2+} uptake in mitochondria and in Ca^{2+}-induced reactions inside mitochondria.

In accordance with numerous observations, the exposure of mitochondria to tBHP considerably enhanced the probability of Ca^{2+}-induced MPT. It was shown earlier that exposure of heart mitochondria to tBHP resulted in peroxidation of cardiolipin, associated with an increased sensitivity of mitochondria to Ca^{2+}-induced MPT (Petrosillo et al. 2009). In our experiments, the oxidant simultaneously increased the rate of mitochondria swelling and decreased the affinity of mitochondria to Ca^{2+}. It was concluded that tBHP oxidizes the vicinal SH-groups of mitochondrial membrane to disulphides, which results in higher gating potential (or higher pore opening probability) (Petronilli et al.1994). Stabilization of the ANT in "c" conformation by oxidative stress inductors (tBHP and diamide) due to reaction with thiol groups was found to increase MPT pore opening in the inner mitochondrial membrane (Castilho et al. 1996; Halestrap and Brenner, 2003; Halestrap 2010; Korotkov et al. 2016). Recently, it has been shown that Ca^{2+}-induced swelling enhanced by tBHP was inhibited by ADP and hydrophobic thiol reagent, *N*-ethylmaleimide, and CsA additionally increased these effects of ADP and *N*-ethylmaleimide (Korotkov et al., 2016). Ca^{2+} release from the damaged mitochondria plays a role in this process because EDTA (0.5 mM) inhibited membrane depolarization induced by tBHP. In our experiments, tBHP oxidizes mitochondrial NADH (at low oxidant concentrations this process was reversible). Earlier we have shown that direct oxidative modification of enzymatic complexes of the respiratory chain and matrix, mitochondrial reduced glutathione depletion, protein glutathionylation, membrane lipid peroxidation, and Ca^{2+}-overload are the main events of mitochondrial peroxidative damages induced by tBHP (Zavodnik et al. 2013). It was suggested that tBHP was reduced directly by cytochrome *c1*, and/or cytochrome *c* of the electron transport chain of rat liver mitochondria and generated methyl, tert-butoxyl- and tert-butylperoxyl- radicals (Kennedy et al. 1992).

On the opposite, the other oxidant, HOCl, at concentrations of 200–300 μM inhibited swelling due to Ca^{2+}-induced MPT (Fig. 1b) and considerably decreased the mitochondrial membrane potential and NADH level in EDTA-free medium. The inhibitory effect depended on both HOCl and Ca^{2+} concentrations. In our earlier work, we showed numerous signs of HOCl-induced mitochondrial dysfunction: hypochlorous acid (50–300 μM) considerably inhibited rat liver mitochondria respiration and the key enzyme of the Krebs cycle, α-ketoglutarate dehydrogenase, produced mitochondrial uncoupling and oxidized mitochondrial protein sulfhydryl groups and glutathione (Maksimchik et al. 2010). HOCl, as was shown earlier, irreversibly oxidized SH-groups to sulphonyl chloride, $R\text{-}SO_2Cl$, without conversion to disulphide (Winterbourn and Brennan 1997) and by this way prevented pore opening. The other mechanism of HOCl-inhibition of pore formation may be the inhibition of the mitochondrial Ca^{2+} uptake due to the decrease of membrane potential caused by HOCl. Using HeLa cells, we determined the dose effect of HOCl on MPT pore opening in intact cell system. HOCl at concentrations of above 15 μM produced pore opening in the whole cell and Ca^{2+} efflux from mitochondria to the cytoplasm (data not shown).

In the earlier works of Bernardi (1992) and Petronilli et al. (1993a, b; 1994), it was suggested that MTP behaves as a voltage-dependent channel modulated by (i) membrane potential in the case of increased pore opening probability upon depolarization, (ii) matrix pH in the case of decreased pore opening probability as the matrix pH drops below 7.0, and (iii) Me^{2+} binding to inner and outer sites independently modulating the pore open–closed transition (Petronilli et al. 1994). The pair of vicinal membrane thiols can be seen as a redox sensor, regulating pore activity (Petronilli et al. 1993a, b; Bernardi 1992; Petronilli et al. 1994).

Conclusions

Rat liver mitochondria exposure to exogenous calcium ions resulted in mitochondrial membrane depolarization and NADH depletion and MPT onset. The apparent Michaelis–Menten constant K_m for Ca^{2+} interaction with mitochondria in the reaction of pore formation, as determined from the Lineweaver–Burk plot of the dependence of MPT rate on Ca^{2+} concentration, is equal to 75 ± 20 μM (at 25 °C), and the apparent $K_d = 60 \pm 12$ μM, as was calculated from the Hill plot of this dependence. This value is higher in comparison with the known K_d for mitochondrial Ca^{2+} uniporter ($K_d = 10$ μM). Three Ca^{2+} ions cooperatively interact with mitochondrial sites (the Hill coefficient $n = 3$). We registered temperature-dependent mitochondria structural transition in the physiological range of 30–34 °C resulting in a significant decrease of activation energy of MPT at higher temperatures. The activation energies of the MPT onset at temperatures lower and above 30–34 °C are calculated to be equal to 130 ± 20 and 50 ± 9 kJ/mol, respectively. The oxidants studied, tBHP and HOCl, reduced mitochondrial membrane potential, and oxidized mitochondrial NADH in the EDTA-free medium.

Acknowledgements This study was partially supported by the grant M13-102 from the Belarusian Republican Foundation for Fundamental Research (to Dr. Ilya Zavodnik). We are grateful to Ms. Lyudmila Kiryukhina for the help in the preparation of the manuscript.

Compliance with Ethical Standards

Conflict of interest The authors declare that they have no conflict of interest.

Informed consent The informed consent was obtained from all the individual participants included in the study.

References

Akerman KEO, Wikström MKF (1976) Safranine as a probe of the mitochondrial membrane potential. FEBS Lett 6:191–197

Alaviana KN, Beutner G, Lazrove E, Sacchetti S, Park H-A, Licznerski P, Li H, Nabili P, Hockensmith K, Graham M, Porter GA Jr, Jonas EA (2014) An uncoupling channel within the c-subunit ring of the F_1F_O ATP synthase is the mitochondrial permeability transition pore. Proc Nat Acad Sci USA 111: 10580–10585.

Armstrong JS, Yang H, Duan W, Whiteman M (2004) Cytochrome *bc1* regulates the mitochondrial permeability transition by two distinct pathways. J Biol Chem 279:50420–50428

Baines CP, Kaiser RA, Sheiko T, Craigen WJ, Molkentin JD (2007) Voltage-dependent anion channels are dispensable for mitochondrial-dependent cell death. Nat Cell Biol 9(5):550–555

Baranov SV, Stavrovskaya IG, Brown AM, Tyryshkin AM, Kristal BS (2008) Kinetic model for Ca^{2+}-induced permeability transition in energized liver mitochondria discriminates between inhibitor mechanisms. J Biol Chem 283:665–676

Bartolomé FA, Abramov Y (2015) Measurement of mitochondrial NADH and FAD autofluorescence in live cells. Methods Mol Biol 1264:263–270

Batandier C, Leverve X, Fontaine E (2004) Opening of the mitochondrial permeability transition pore induces reactive oxygen species production at the level of the respiratory chain complex I. J Biol Chem 279:17197–17204

Battaglia V, Grancara S, Satriano J, Saccoccio S, Agostinelli E, Toninello A (2010) Agmatine prevents the Ca(2+)-dependent induction of permeability transition in rat brain mitochondria. Amino Acids 38:431–437

Bellomo G, Jewell SA, Thor H, Orrenius S (1982) Regulation of intracellular calcium compartmentation: studies with isolated hepatocytes and t-butyl hydroperoxide. Proc Natl Acad Sci USA 79:6842–6846

Bernardi P (1992) Modulation of the mitochondrial cyclosporin A-sensitive permeability transition pore by the proton electrochemical gradient. Evidence that the pore can be opened by membrane depolarization. J Biol Chem 267:8834–8839

Bernardi P (2013) The mitochondrial permeability transition: a mystery solved?. Front Physiol 495:1–12.

Bernardi P, Di Lisa F (2015) The mitochondrial permeability transition pore: Molecular nature and role as a target in cardioprotection. J Mol Cell Cardiol 78:100–106

Bernardi P, Rasola A, Forte M, Lippe G (2015) The mitochondrial permeability transition pore: channel formation by F-ATP synthase, integration in signal transduction, and role in pathophysiology. Physiol Rev 95:1111–1155

Bernardi P, Veronese P, Petronilli V (1993) Modulation of the mitochondrial cyclosporin A-sensitive permeability transition pore. I. Evidence for two separate Me^{2+} binding sites with opposing effects on the pore open probability. J Biol Chem 268(2):1005–1010

Byrne AM, Lemasters JJ, Nieminen AL (1999) Contribution of increased mitochondrial free Ca^{2+} to the mitochondrial permeability transition induced by tert-butylhydroperoxide in rat hepatocytes. Hepatology 29:1523–1531

Castilho RF, Kowaltowski AJ, Vercesi AE (1996) The irreversibility of inner mitochondrial membrane permeabilization by Ca^{2+} plus prooxidants is determined by the extent of membrane protein thiol cross-linking. J Bioenerg Biomembr 28:523–539

Davies JM, Horwitz DA, Davies KJ (1993) Potential roles of hypochlorous acid and N-chloroamines in collagen breakdown by phagocytic cells in synovitis. Free Radic Biol Med 15:637–643

Drahota Z, Kriváková P, Cervinková Z, Kmoníčková E, Lotková H, Kucera O, Houstek J (2005) Tert-butyl hydroperoxide selectively inhibits mitochondrial respiratory-chain enzymes in isolated rat hepatocytes. Physiol Res 54:67–72

Duchen MR (2004) Mitochondria in health and disease: perspectives on a new mitochondrial biology. Rev Mol Aspects Med 25:365–451

Favero TG, Colter D, Hooper PF, Abramson JJ (1998) Hypochlorous acid inhibits Ca(2+)-ATPase from skeletal muscle sarcoplasmic reticulum. J Appl Physiol 84:425–430

Feissner RF, Skalska J, Gaum WE, Sheu SS (2009) Crosstalk signaling between mitochondrial Ca2+ and ROS. Front Biosci (Landmark 14: 1197–1218

Forte M, Bernardi P (2005) Genetic dissection of the permeability transition pore. J Bioenerg Biomembr 37:121–128

Giorgio V, Stockum S, Antoniel M, Fabbro A, Fogolari F, Forte MA, Glick GD, Petronilli V, Zoratti M, Szabo I, Lippe G, Bernardi P (2013) Dimers of mitochondrial ATP synthase form the permeability transition pore. PNAS 110(15):5887–5892

Halestrap AP (2010) A pore way to die: the role of mitochondria in reperfusion injury and cardioprotection. Biochem Soc Trans 38:841–860

Halestrap AP (2014) The c ring of the $F1F_0$ ATP synthase forms the mitochondrial permeability transition pore: a critical appraisal. Front Oncol 4:234

Halestrap AP, Brenner C (2003) The adenine nucleotide translocase: a central component of the mitochondrial permeability transition pore and key player in cell death. Curr Med Chem 10:1507–1525

Halestrap AP, Connern CP, Griffiths EJ, Kerr PM (1997) Cyclosporin A binding to mitochondrial cyclophilin inhibits the permeability transition pore and protects hearts from ischaemia/reperfusion injury. Mol Cell Biochem 174:167–172

Halestrap AP, Woodfield KY, Connern CP (1997) Oxidative stress, thiol reagents, and membrane potential modulate the mitochondrial permeability transition by affecting nucleotide binding to the adenine nucleotide translocase. J Biol Chem 272:3346–3354

Hawkins BJ, Levin MD, Doonan PJ, Petrenko NB, Davis CW, Patel VV, Madesh M (2010) Mitochondrial Complex II prevents hypoxia but not calcium- and proapoptotic Bcl-2 protein-induced mitochondrial potential loss. J Biol Chem 285:26494–26505

Johnson D, Lardy HA (1967) Isolation of liver or kidney mitochondria. Meth Enzymol 10:94–101.

Jonas EA, Porter CA Jr, Beutner G, Mnatsakanyan N, Alavian K (2015) Cell death disguised: the mitochondrial permeability transition pore as the c-subunit of the F1FO ATP synthase. Pharmacol Res 99:382–392

Kennedy CH, Church DF, Winston GW, Pryor WA (1992) tert-Butyl hydroperoxide-induced radical production in rat liver mitochondria. Free Radic Biol Med 12:381–387

King M, Jefferson E (1997) Secretion and inactivation of myeloperoxidase by isolated neutrophils. J Leukoc Biol 61:293–302

Kokoszka JE et al (2004) The ADP/ATP translocator is not essential for the mitochondrial permeability transition pore. Nature 427(6973):461–465)

Korotkov SM, Konovalova SA, Brailovskaya IV, Saris NEL (2016) To involvement the conformation of the adenine nucleotide translocase in opening the Tl^{+}-induced permeability transition pore in Ca^{2+}-loaded rat liver mitochondria. Toxicol Vitro 32: 320–332.

Kowaltowski AJ, Castilho RF, Vercesi AE (2001) Mitochondrial permeability transition and oxidative stress. FEBS Lett 495:12–15

Krauskopf A, Eriksson O, Craigen WJ, Forte MA, Bernardi P (2006) Properties of the permeability transition in VDAC1–/– mitochondria. Biochim Biophys Acta 1757(5–6):590–595

Kriváková P, Lábajová A, Cervinková Z, Drahota Z (2007) Inhibitory effect of t-butyl hydroperoxide on mitochondrial oxidative phosphorylation in isolated rat hepatocytes. Physiol Res 56:137–140

Kushnareva YE, Sokolova PM (2000) Prooxidants open both the mitochondrial permeability transition pore and a low-conductance channel in the inner mitochondrial membrane. Arch Biochem Biophys 376(2):377–388

Lapidus RG, Sokolove PM (1994) The mitochondrial permeability transition. Interactions of spermine, ADP, and inorganic phosphate. J Biol Chem 269:18931–18936

Leung AW, Halestrap AP (2008) Recent progress in elucidating the molecular mechanism of the mitochondrial permeability transition pore. Biochim Biophys Acta 1777:946–952.

Lowry OH, Rosebrough NJ, Farr AL, Randall RJ (1951) Protein measurement with the Folin phenol reagent. J Biol Chem 193:265–275

Maksimchik YZ, Dremza IK, Lapshina EA, Cheshchevik VT, Sudnikovich EJu, Zabrodskaya SV, Zavodnik IB (2010) Rat liver mitochondria impairments under acute carbon tetrachloride-induced intoxication. Effects of melatonin. Biochem (Moscow) Suppl Ser A 4: 187–195.

Marsh D (1992) Analysis of the bilayer phase transition temperatures of phosphatidylcholines with mixed chains. Biophys J 61:1036–1040

McStay GP, Clarke SJ, Halestrap AP (2002) Role of critical thiol groups on the matrix surface of the adenine nucleotide translocase in the mechanism of the mitochondrial permeability transition pore. Biochem J 367:541–548

Moore AL, Bonner WD (1982) Measurements of membrane potentials in plant mitochondria with the safranine method. Plant Physiol 70:1271–1276

Nieminen AL, Byrne AM, Herman B, Lemasters JJ (1997) Mitochondrial permeability transition in hepatocytes induced by t-BuOOH: NAD(P)H and reactive oxygen species. Am J Physiol 272:1286–1294

Orrenius S, Zhivotovsky B, Nicotera P (2003) Regulation of cell death: the calcium-apoptosis link. Nat Rev Mol Cell Biol 4:552–565

Pandya JD, Nukala VN, Sullivan PG (2013) Concentration dependent effect of calcium on brain mitochondrial bioenergetics and oxidative stress parameters. Front Neuroenergetics 5:10.

Patergnani S, Suski JM, Agnoletto C, Bononi A, Bonora M, De Marchi E, Giorgi C, Marchi S, Missiroli S, Poletti F, Rimessi A, Duszynski J, Wieckowski MR, Pinton P (2011) Calcium signaling around Mitochondria Associated Membranes (MAMs). Cell Commun Signal 9:19–28.

Peng TI, Jou MJ (2010) Oxidative stress caused by mitochondrial calcium overload. Ann N Y Acad Sci 1201:183–188

Petronilli V, Cola C, Bernardi P (1993a) Modulation of the mitochondrial cyclosporin A-sensitive permeability transition pore. II. The minimal requirements for pore induction underscore a key role for transmembrane electrical potential, matrix pH, and matrix Ca^{2+}. J Biol Chem 268:1011–1016

Petronilli V, Cola C, Massari S, Colonna R, Bernardi P (1993b) Physiological effectors modify voltage sensing by the cyclosporine A-sensitive permeability transition pore of mitochondria. J Biol Chem 268:21939–21945

Petronilli V, Costantini P, Scorrano L, Colonna R, Passamonti S, Bernardi P (1994) The voltage sensor of the mitochondrial permeability transition pore is tuned by the oxidation-reduction state of vicinal thiols. Increase of the gating potential by oxidants and its reversal by reducing agents. J Biol Chem 269:16638–16642

Petrosillo G, Moro N, Ruggiero FM, Paradies G (2009) Melatonin inhibits cardiolipin peroxidation in mitochondria and prevents the mitochondrial permeability transition and cytochrome c release. Free Radic Biol Med 47:969–974

Petrosillo G, Ruggiero FM, Pistolese M, Paradies G (2004) Ca^{2+}-induced reactive oxygen species production promotes cytochrome c release from rat liver mitochondria via mitochondrial permeability transition (MPT)-dependent and MPT-independent mechanisms: role of cardiolipin. J Biol Chem 279:53103–53108

Richardson AP, Halestrap AP (2016) Quantification of active mitochondrial permeability transition pores using GNX-4975 inhibitor titrations provides insights into molecular identity. Biochem J 473(9):1129–1140

Rizzuto R, De Stefani D, Raffaello A, Mammucari C (2012) Mitochondria as sensors and regulators of calcium signalling. Nat Rev Mol Cell Biol 13:566–578

Santo-Domingo J, Demaurex N (2010) Calcium uptake mechanisms of mitochondria. Biochim Biophys Acta 1797:907–912.

Whiteman M, Rose P, Siau JL, Cheung NS, Tan GS, Halliwell B, Armstrong JS (2005) Hypochlorous acid-mediated mitochondrial dysfunction and apoptosis in human hepatoma HepG2 and human fetal liver cells: role of mitochondrial permeability transition. Free Radic Biol Med 38:1571–1584

Winterbourn CC, Brennan SO (1997) Characterization of the oxidation products of the reaction between reduced glutathione and hypochlorous acid. Biochem J 326:87–92

Yang YT, Whiteman M, Gieseg SP (2012) HOCl causes necrotic cell death in human monocyte derived macrophages through calcium dependent calpain activation. Biochim Biophys Acta 1823:420–429.

Zamzami N, Kroemer G (2001) The mitochondrion in apoptosis: how Pandora's box opens. Nat Rev Mol Cell Biol 2:67–71

Zavodnik IB, Dremza IK, Cheshchevik VT, Lapshina EA, Zamaraewa M (2013) Oxidative damage of rat liver mitochondria during exposure to t-butyl hydroperoxide. Role of Ca^{2+}—ions in oxidative processes. Life Sci 92:1110–1117